Macromolecules **1986**, *19*, 1021–1029 **1021**

(34) Rinaldi, P. L. *J. Am. Chem. Soc.* **1983**, *105*, 5165.
(35) Benn, R.; Günther, H., *Angew. Chem., Int. Ed. Engl.* **1983**, *22*, 350.
(36) Maudsley, A. A.; Muller, L.; Ernst, R. R. *J. Magn. Reson.* **1977**, *28*, 463.
(37) Bodenhausen, G.; Freemen, R. *J. Magn. Reson.* **1977**, *28*, 471.
(38) It should be noted that the definition of τ_c itself may be ambiguous. In any event, for this structural class of polymers, overall polymer motion in these concentrated solutions is slow relative to ω_0.

Poly(vinyl acetate) Dynamics Studied by Proton and Carbon-13 Nuclear Magnetic Resonance in the Solid State

S. Ganapathy,[†] V. P. Chacko,[‡] and R. G. Bryant*[†]

Departments of Radiology, Biophysics, and Chemistry, University of Rochester, Rochester, New York 14642, and Department of Radiology, Johns Hopkins Medical Center, Baltimore, Maryland 21025. *Received October 7, 1985*

ABSTRACT: Carbon and proton nuclear magnetic resonance measurements have been applied to the poly(vinyl acetate) system in the presence and absence of water. Proton magnetic relaxation dispersion measurements from 0.01 to 30 MHz demonstrate a low-frequency dispersion that indicates a distribution of low-frequency motions that drive the proton magnetic relaxation. The static carbon spectra demonstrate that the carboxyl side-chain region of the polymer is largely unaffected by the addition of water. However, there are dramatic changes in the carbon spin–lattice relaxation rates when the polymer is hydrated. In the presence of water the carbon spin–lattice relaxation is dominated by the high-frequency motion of the water molecules, but carbon relaxation and proton relaxation in the rotating frame are controlled by slower polymer motions of sufficiently small amplitude that the carboxyl carbon chemical shift tensor is largely unaffected.

Introduction

The interaction between water molecules and motions in macromolecular systems is important for understanding materials properties, and in the case of biological catalysts, the details of function and mechanism. Biologically critical molecules such as enzyme catalysts are difficult to study because the considerable monomer heterogeneity produces very complex spectra; simpler polymeric systems may, therefore, serve as reasonable model systems for deducing main dynamical principles, but which are of considerable interest in their own right. The present report concerns the dynamical response of a polymer to the addition of water. Poly(vinyl acetate) was chosen as a model system because of its convenient spectroscopic and physical properties. The monomeric unit is shown in Figure 1.

Motions in polymeric solids have been studied by magnetic resonance methods for a number of years using highly sensitive proton magnetic resonance methods. Attempts are often made to relate the physical properties of the polymer to the proton spin–lattice relaxation times in the laboratory and rotating frames, T_1^{H} and $T_{1\rho}^{\mathrm{H}}$. A major difficulty with detailed interpretation of proton spin parameters arises because of efficient spin–spin communication between protons in different regions of the polymer, i.e., spin diffusion, which often averages the effects of local dynamical heterogeneity. Nevertheless, such studies have shown clearly that at temperatures below the glass transition temperature, T_g, local motions such as side-chain motions, terminal group rotations, or main-chain local fluctuations dominate the observed nuclear magnetic relaxation behavior, but at temperatures above T_g, backbone motions contribute importantly.[1,2]

It is well-known that the addition of solvent or plasticizer to a glassy polymer lowers T_g, changes the mechanical properties, and is a function of the particular polymer–plasticizer interaction.[3–7] Though there have been a number of NMR studies on polymer dynamics, there have been relatively few that examine the dynamical effects of polymer–solvent interactions. The emergence of high-resolution rare-spin magnetic resonance methods in solids such as cross-polarization[8] magic angle sample spinning[9,10] (CP–MASS) combined with strong dipolar decoupling[11] permits observation of particular monomer carbon resonances, thus providing the possibility of site-specific resolution in an analysis of the polymer dynamics.[12] In glassy polymers there is some broadening of the polymer carbon spectrum obtained under magic angle spinning conditions;[12] however, the resolution is sufficient to resolve all four carbon resonances in poly(vinyl acetate), permitting independent measurement of relaxation rates and in some cases line shapes in nonspinning samples. Since the rare spin is not subject to the relaxation averaging associated with efficient spin diffusion, the carbon spectrum offers site-resolved nuclear magnetic relaxation times. The main parameters that are available include the carbon-13 line shape, the proton relaxation times T_1^{H} and $T_{1\rho}^{\mathrm{H}}$, and the carbon relaxation times T_1^{C} and $T_{1\rho}^{\mathrm{C}}$, all sampling somewhat different spectral densities, thus permitting a dynamical characterization that reflects motions at different frequencies.

Earlier work on poly(vinyl acetate) using high-resolution solution-phase NMR methods has shown that water is a poor solvent;[6] however, saturation of the polymer with water lowers the glass transition temperature by 25 °C. Further, it was shown that high-resolution carbon NMR spectra could be obtained at temperatures about 100 °C above T_g using radio-frequency (rf) levels appropriate to scalar decoupling of the protons; however, detailed analysis of polymer motions and the contributions of water were not reported. Here we report an extensive data set on both wetted and dry polymer. We address the contribution of water to both the carbon and proton magnetic relaxation in wetted poly(vinyl acetate) and use the carbon line shape, the carbon relaxation times T_1^{C} and $T_{1\rho}^{\mathrm{C}}$, and the field dependence of the proton relaxation time T_1^{H} to partially characterize the motions in the system.

[†] University of Rochester.
[‡] Johns Hopkins Medical Center.

0024-9297/86/2219-1021$01.50/0 © 1986 American Chemical Society

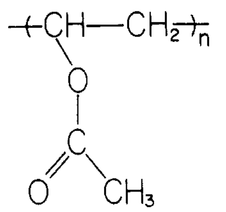

Figure 1. Monomeric unit of poly(vinyl acetate) showing the four resolvable carbon atoms.

Experimental Section

Poly(vinyl acetate) obtained from Polysciences Inc. was supplied by Professor W. G. Miller, University of Minnesota. The polymer was amorphous and atactic, had a weight-average molecular weight of 1.9×10^5, and was used without further purification. Dry samples of the polymer were prepared by drying beads of the polymer in vacuo over boiling acetone for several hours and then packing into 10-mm sample tubes. The water content in the dry samples was estimated to be less than 1% by weight.

Treatment of the polymer with water produces physically different samples, depending on the method of preparation. When the polymer was allowed to stand in the presence of excess water for several weeks and the remaining excess water simply pressed out, the sample was biphasic and similar to that used by Professor Miller and co-workers in their study.[6] This sample is dynamically heterogeneous as will be shown. On spinning this sample in a high-speed rotor at 2 kHz, excess water on the polymer is spun out. Depending on the length of the spinning run, the resulting material may lose the dynamical heterogeneity. The polymer remains hydrated, however, and was found to contain between 6 and 9% water by weight.

The proton spin–lattice relaxation times were measured as a function of magnetic field strength in the range corresponding to Larmor frequencies from 0.01 to 30 MHz on a field-cycling spectrometer built in this laboratory with the collaboration of Dr. Seymour Koenig and Dr. Rodney Brown, III, and described elsewhere.[13] The magnetic field was cycled between a fixed soak field of 0.705 T and a measure field varying between 23.5 mT and 0.94 T; a fixed resonance field of 0.493 T was used. The proton magnetization amplitude was measured on the proton FID following a 90° pulse after the resonance field was achieved, captured by a sample and hold circuit, and digitized by an IBM 7406 device coupler. On-line least-squares fits were made on the relaxation data. The temperature of the sample was 287 K and was maintained by a liquid cooling system using freon as the cryogenic fluid.

All carbon-13 measurements were made on a solids spectrometer built in this laboratory, described in detail elsewhere,[14] and operating at 56.44 MHz for protons and 14.19 MHz for carbon. Carbon spectra were obtained by cross-polarization with magic angle spinning at 2 kHz when desired. The CP was established by using a single-contact Hartmann–Hahn match[15] at approximately 40 kHz rf field. The contact time for polarization transfer was chosen to be 1 ms for the dry sample and 0.5 ms for the wet samples. Proton decoupling was maintained at 60 kHz or greater for 50 ms and the efficiency of the high-power decoupling was often checked with a spinning sample of 3-methylglutaric acid.

For carbon T_1 measurements, the carbon magnetization obtained by cross-polarization along the x' direction was subsequently rotated by a 90° pulse to lie along the $-z'$ direction using a carbon pulse applied along the y' direction. After a variable time τ during which the proton rf was turned off, a carbon 90° pulse was applied along the y' direction and the resulting FID was sampled under strong proton decoupling. Typically 1000 transients were accumulated and the resulting FID was Fourier transformed. Least-squares analysis of the decay of the individual carbon signal intensities as a function of the delay time yielded the relaxation time.[16] Nonexponentiality in the decay was not observed. Since in our measurements $T_1^H \ll T_1^C$, there was no need to irradiate the protons during the delay time to suppress the transient nuclear Overhauser effects.[17]

Measurements of carbon spin–lattice relaxation in the rotating frame were made by creating the transverse carbon magnetization by a cross-polarization contact with the protons followed by maintenance of the spin-locked carbon magnetization for a variable time τ along the applied carbon rf field of chosen amplitude, ν_{1C}, during which the proton decoupling field was turned off. At the end of the delay time, the carbon FID was sampled with the strong proton decoupling field on; typically 1000 transients were accumulated. The logarithm of the individual carbon resonance intensity was plotted against the spin-locking time to yield the effective rotating frame relaxation time, $T_{1\rho}^{C*}$. The measurements were repeated for different ν_{1C} values in the range 25–98 kHz. The spin-locking field strength was calibrated with an external hexamethylbenzene sample under identical conditions by measuring the length of a 4π pulse.

For the carbon cross-polarization spectra of static samples, the temperature at the sample was controlled to within 3 °C with a Varian temperature control unit. All the CP–MASS carbon relaxation time measurements were made at ambient temperature between 294 and 298 K. The glass transition temperature for dry poly(vinyl acetate) is 302 K.[6]

Results and Discussion

Proton Relaxation Dispersion. The proton spin–lattice relaxation rates are shown as a function of magnetic field strength, plotted as the proton Larmor frequency, in Figure 2A for dry poly(vinyl acetate). The proton relaxation dispersion behavior shows that there is a strong magnetic field dependence of the observed relaxation rate at Larmor frequencies below 200 kHz. Within the sampling constraints of the field-cycling spectrometer, the proton relaxation is characterized by a single-exponential time constant over the frequency range studied. A typical result is shown in Figure 2B.

The observation of a single-exponential decay of the proton magnetization provides evidence that the polymer is sufficiently homogeneous that there are no barriers to efficient proton spin diffusion; i.e., the polymer protons are characterized by a single spin temperature and relax as a single well-mixed magnetic system. The monotonic smooth increase in relaxation rate at lower frequencies reflects the existence of low-frequency motions. The relaxation dispersion observed cannot be explained by motion of the methyl group, though methyl group rotation is a common feature in polymer spin relaxation.[1,2] Previous work has clearly demonstrated that the methyl rotation is extremely rapid at the temperatures studied here, leading to a magnetic relaxation dispersion at frequencies in the hundreds of megahertz range, which are inaccessible on our equipment. The observed relaxation dispersion thus reflects motions other than methyl rotation.

If one assumes (1) that spin–lattice relaxation is caused by random molecular motions within the monomeric unit with distinct correlation times τ_c^i, (2) that there is no correlation or interference between the motions, and (3) that all the polymer chains come to a common spin temperature by spin diffusion, the field dependence of the relaxation is implied by the equation

$$\frac{1}{T_1^H} = \sum_i C_i \left[\frac{\tau_c^i}{1 + (\omega_{0H}\tau_c^i)^2} + \frac{4\tau_c^i}{1 + (2\omega_{0H}\tau_c^i)^2} \right] \quad (1)$$

where ω_{0H} is the proton Larmor frequency and C_i represents the strength of the relaxation interaction associated with the ith motion with correlation time τ_c^i. Equation 1 is an extension of the well-known relaxation equations[18] to several independent relaxation processes where the motions are uncorrelated; it is approximate in that the motional anisotropy, which clearly is present in any such constrained system, is not explicitly included, but reflected in C. Other relaxation equations derived for the case of highly anisotropic motion may be appropriate as well.[19] Application of eq 1 with two terms, one for methyl rotation, permits motional characterization of the low-frequency

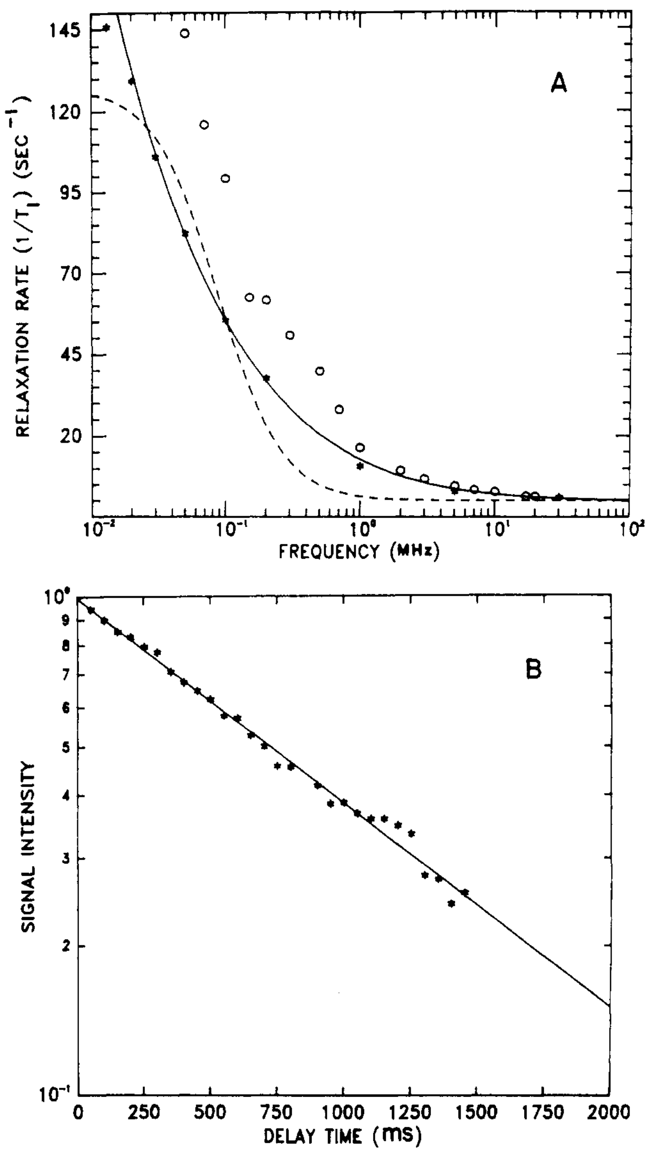

Figure 2. (A) Proton spin–lattice relaxation rate measured as a function of magnetic field strength, indicated as proton Larmor frequency, for dry (*) and wet (O) poly(vinyl acetate) obtained at 287 K. The dashed line represents the fit to the dry data assuming a single correlation time model for the motions using eq 1 with $C = 1 \times 10^{10}$ s^{-2} and $\tau_g = 1 \times 10^{-12}$ s for methyl rotation and $C = 2.5 \times 10^7$ s^{-2} and $\tau_c = 1 \times 10^{-6}$ s for the low-frequency motions. The solid line is calculated assuming a log χ^2 distribution of correlation times with the parameters $b = 1000$, $p = 7$, and $\bar{\tau} = 1 \times 10^{-8}$ s (see ref 20). (B) Representative plot of the proton longitudinal magnetization decay (*) obtained at a measure field of 0.013 MHz for dry poly(vinyl acetate). The solid line represents a linear least-squares fit to the data to yield T_{1H}.

dispersion; the dashed line results, which is clearly a poor fit to the data. There are several interpretative options. The solid line in Figure 2A was obtained by fitting the data with a log χ^2 distribution of correlation times with the parameters shown in the caption. The fit and the choice of distribution function are not unique, though the shape of this asymmetric function appears justified.[20] We point out only that some distribution of motions is required to fit the data and that the proton relaxation rate does not plateau at the lowest frequencies shown. It might be expected that the lowest effective field possible in this experiment is H_{local}; thus the highest rate would be $1/T_{1D}{}^{H}$.

We have independently measured $1/T_{1D}{}^{H}$ of dry poly(vinyl acetate) at 56.4-MHz resonance field for protons using the Jeener–Broekaert sequence[21] and found that the

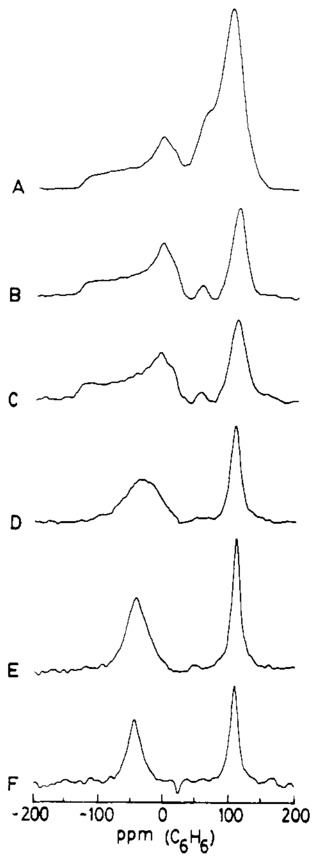

Figure 3. Static carbon-13 cross-polarization spectra of poly(vinyl acetate) obtained at 14.2 MHz at ambient probe temperature: (A) dry sample with no dipolar dephasing delay; (B) cross-polarization spectrum with a 40-μs dipolar dephasing delay prior to data acquisition on a dry sample; (C) cross-polarization spectrum with a 40-μs dipolar dephasing delay on the wet sample which had been spun at approximately 2 kHz to remove excess water; (D–F) similar dipolar dephased spectra taken on a wet sample containing excess water (biphasic) with recycle times of 2 s for (D), 1 s for (E), and 0.7 s for (F).

dipolar signal decays biexponentially with rates of 77 and 1.4×10^4 s^{-1}. The slower decay rate for the dipolar signal is smaller than the spin–lattice relaxation rate measured at the lowest magnetic fields using the relaxation dispersion spectrometer. The difference is consistent with the terms in the equation for the dipolar relaxation rate, which may usually be neglected at high field but become important at the lowest fields measured, elevating the relaxation rate compared with the high-field values.[22] In addition, the motions in the polymer may decrease the effective dipolar field strength, thus shifting the plateau off scale to the left in Figure 2A.

The proton relaxation dispersion for poly(vinyl acetate) hydrated with water is shown in Figure 2A as well. In the wet sample the relaxation rate is nearly doubled at all magnetic field strengths, and as in the dry sample, there is a clear dispersion in the relaxation rate in the low-frequency region, 40–100 kHz. It is unclear from just the proton measurements whether the relaxation rate change is due to motion of the water protons behaving as relaxation sinks or due to water molecules stimulating the motion of the polymer. Since the carbon data to be presented will show that this sample is not essentially homogeneous, we have not attempted to fit the data with a distribution of correlation times.

Carbon Line Shapes. Carbon cross-polarization NMR spectra are shown in Figure 3 for dry and water-treated poly(vinyl acetate) obtained with several data acquisition

Table I
Poly(vinyl acetate) ^{13}C Spectral and Relaxation Data

parameter	dry	wet[a]
$\bar{\sigma}$(COO)[b]	$\sigma_{11} = -127$ $\sigma_{22} = -8$ $\sigma_{33} = +15$	$\sigma_{11} = -138$ $\sigma_{22} = -11$ $\sigma_{33} = +3$

	dry				wet[a]			
parameter	COO	CH	CH_2	CH_3	COO	CH	CH_2	CH_3
σ_{MASS}	−41.3	+61.6	+89.2	+108.0	−41.2	+61.6	+89.5	+108.0
T_1^C, s	30	20	18	13	9	2	1	4
					(28)	(12)	(11)	(11)
$T_{1\rho}^C$,[c] ms	170	43	37	89	33	3	4	12
					(37)	(9)	(7)	(27)[d]

[a] Wet corresponds to the polymer hydrated with H_2O as described in the text. Where measurements were taken for D_2O-treated sample, results are shown in parentheses. [b] Chemical shifts are expressed in ppm with respect to external benzene. [c] At ν_{1C} = 91 kHz. [d] At ν_{1C} = 80 kHz.

methods. Figure 3A shows significant spectral overlap in the sp^2-carbon region because of main-chain resonances that may be largely eliminated by using a correctly chosen dipolar dephasing delay.[23] The resulting spectra shown in Figure 3B–F exhibit well-resolved sp^2-carbon line shapes. The effect of varying the recycle time of the CP experiment on the observed carbon line shape is displayed in Figure 3D–F for the water-saturated poly(vinyl acetate). In bulk polymer the carboxyl carbon line shape corresponds to an asymmetric tensor with a large chemical shielding anisotropy similar to those found in simple acetates and other closely related systems.[14] The observed singularities in the powder pattern for the sp^2 carbon lead to the principal values of the chemical shielding tensor shown in Table I. The sp^2-carbon tensor is sensitive to changes in local environment, but the sharpness of the powder pattern at the singularities demonstrates that there is no appreciable distribution in the principal values of the tensor, which suggests that the polymer is structurally fairly homogeneous. These tensor components are very near rigid-lattice values in Figures 3A–C, and, therefore, the side-chain motion sensed at the sp^2 carbon is of such small amplitude that significant averaging of the tensor does not result.

The effects of varying the sample temperature on the observed carbon-13 spectra of dry poly(vinyl acetate) are shown in Figure 4. The static carbon spectra change considerably from an almost rigid-lattice line shape at room temperature to a strongly averaged or almost isotropic line shape at approximately 380 K. Both the side-chain and main-chain carbons exhibit continued narrowing of the powder patterns with increasing temperature. It is clear that regardless of the detailed dynamical events or models used to describe them, a temperature rise over this range leads to both main-chain and side-chain motions that average the chemical shift tensors. In the lower temperature range, up to approximately 330 K (see Figure 4), the powder pattern for the sp^2 carbon is maintained though there are clearly some changes in detail. As the temperature is increased further, above about 350 K, the motions apparently become nearly isotropic, though we have not modeled the effects of a broad distribution of correlation times on the powder pattern line shapes.[51] The protons were strongly decoupled in obtaining the spectra in Figure 4; thus, motional averaging of the chemical shielding anisotropy alone is monitored by the line shape. However, at temperatures above 350 K, considerable averaging of the carbon–proton dipolar interaction undoubtedly occurs as shown by the loss of signal to noise in the cross-polarization spectrum shown at the top of Figure 4. This temperature dependence is consistent with the observations of Miller and co-workers, who reported high-resolution carbon-13 spectra in similar samples using only proton scalar decoupling levels at high temperatures.[6] Similar observations have been made on other rubbery polymers well above the glass transition temperature.[24] Comparison of the carboxyl portion of the carbon spectrum for dry poly(vinyl acetate) at 329 K (Figure 4) and poly(vinyl acetate) with excess water at 296 K (Figure 3D) shows that the line shapes are similar for these two samples, which are both approximately 25 K above the glass transition temperature. We have not attempted to fit the carbon line shapes to a detailed motional model.

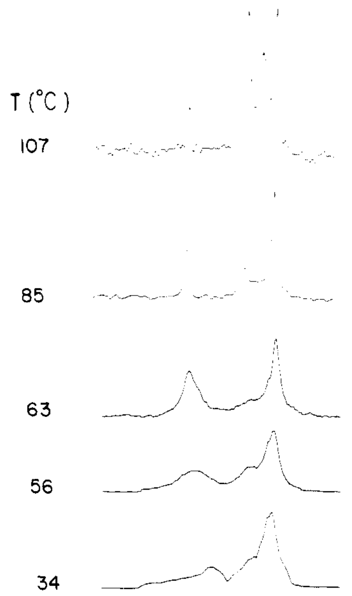

Figure 4. Carbon-13 cross-polarization NMR spectra taken at 14.2 MHz for dry poly(vinyl acetate) at different temperatures.

When poly(vinyl acetate) is saturated and stands in excess water, significant changes are observed in the carbon spectrum as shown in Figure 3D–F. Here the sample is clearly heterogeneous and is apparently similar to that used by Miller and co-workers in their carbon NMR study.[6] The carbon spectra are independent of the amount of excess water as long as the sample is biphasic. It is clear that when the recycle time of the CP experiment is varied, the observed carbon line shapes change and considerable narrowing of the resonances attend the shorter recycle times. When long recycle times are used (2 s), the sp^2-carbon region shows a motionally modified line shape different from that observed for the dry polymer, but at short recycle times the same region of the spectrum is narrowed by a factor of 8 (Figure 3F), demonstrating that the polymer is dynamically heterogeneous in the presence

Table II
"Best-Fit" Parameters to Contact Time Study of Poly(vinyl acetate)[a]

	dry				wet[b]			
parameter	COO	CH	CH_2	CH_3	COO	CH	CH_2	CH_3
T_{IS}, μs	424	74	71	151	497 (403)	62 (35)	37 (27)	111 (112)
$T_{1\rho}{}^{H}$, ms	39.1	46.5	45.2	45.8	5.9 (8.5)	8.4 (9.9)	7.1 (9.9)	8.4 (9.5)
τ_m, μs	1940	478	459	866	1343 (1326)	307 (198)	196 (160)	487 (503)
I_{τ_m}/I_0	0.952	0.990	0.990	0.981	0.796 (0.859)	0.964 (0.945)	0.973 (0.984)	0.944 (0.948)

[a] "Best-fit" values obtained by nonlinear least-squares fit of the contact time study data using eq 2 (see text). [b] Values in parentheses are for D_2O-treated sample. Wet corresponds to the polymer hydrated as described in the text.

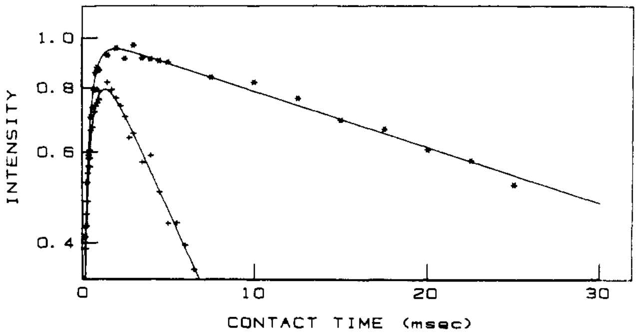

Figure 5. Evolution of the carbon-13 cross-polarization intensity of the sp^2 carbon obtained under matched Hartmann–Hahn condition with magic angle spinning for dry (*) and wet (+) poly(vinyl acetate). The solid line represents the contact time variation given by eq 2 using the best-fit parameters shown in Table II.

of excess water. The resulting carbon line shape is thus a superposition of different motionally averaged components, each of which is modified from that of a rigid sp^2 tensor depending on the details of the motions present in that particular microscopic domain. The local dynamics are clearly sensitive to solvent penetration.[6] It should be noted that selection of spectral components by this type of relaxation rate weighting does not depend on the orientation dependence of the proton longitudinal relaxation rate itself because rapid spin diffusion within each microscopic polymer domain averages the relaxation rates over the orientations in the domain. These observations demonstrate that in this dynamically heterogeneous system there is inefficient proton spin communication between dynamical domains and that in spite of considerable motion in some, there remains sufficient order to provide reasonably efficient cross-polarization from the proton to the carbon spins. For the dry polymer where extensive motional averaging of the carbon-13 line shapes occurs at elevated temperatures, there is no evidence for dynamical heterogeneity in the carbon spectra. It may be noted that although addition of water lowers the glass transition temperature, the carbon-13 line shape at the same relative temperature ($T - T_g$) is similar.

When excess water is removed from the sample by mechanical spinning at 2 kHz, small changes occur in the carbon spectrum. The carboxyl carbon displays a powder pattern characteristic of a rigid tensor, Figure 3C. For this wetted, but not overly saturated system, the sp^2-carbon line shape is independent of the recycle time; thus, the sample is dynamically homogeneous by this measure. Though there are no large changes observed in the carbon line shapes for these samples, there are very dramatic changes in the relaxation times for the carbon atoms when water is added to the system.

Well-resolved carbon-13 resonances are observed for both main-chain and side-chain carbon atoms when the sample is rotated at the magic angle. Within the resolution permitted by the residual line widths for dry and wet poly(vinyl acetate), the isotropic chemical shifts measured were the same (Table I). Thus, the local electronic environments sensed at the carbon sites remain very largely unaltered by the addition of water.

Carbon-13 Cross-Polarization. The effect of varying the contact time on the observed cross-polarization spectra of dry and wet poly(vinyl acetate) was studied under magic angle spinning conditions, permitting the observation of the time evolution of each carbon resonance in the monomer unit. The wet samples were hydrated but not biphasic as shown by an unaveraged static shift tensor of the sp^2 carbon. The data for the sp^2 carbon shown in Figure 5 demonstrate the early growth of magnetization due to the cross-polarization and the long-time decay due mainly to the finite proton spin relaxation time in the rotating frame. The behavior for other carbon resonances was similar. The time evolution of the carbon signal may be satisfactorily described by[25]

$$I(\tau) = \frac{I_0}{1 - \lambda}[1 - e^{-(1-\lambda)\tau/T_{IS}}]e^{-1/T_{1\rho}{}^{H}} \qquad (2)$$

where $\lambda = T_{IS}/T_{1\rho}{}^{H}$ and the rate constants for the growth and decay of the carbon signal are denoted T_{IS} and $T_{1\rho}{}^{H}$, respectively. The data for each carbon atom were analyzed with this equation and the best-fit values of T_{IS} and $T_{1\rho}{}^{H}$ are summarized in Table II. Figure 5 indicates the quality of the fit.

These data demonstrate that the addition of water reduces the proton $T_{1\rho}$ fourfold when the polymer is hydrated, but there is little effect on the cross-polarization rate. The value of the contact time that yields the optimal signal is given by

$$\tau_m = \frac{T_{IS}}{1 - \lambda} \ln (1/\lambda) \qquad (3)$$

These contact times and the fractional decrease in the maximal signal intensity from I_0 are compared for wet and dry samples in Table II. Since the cross-polarization parameter does not change very much on hydration of the polymer, the shift in the optimal contact time is mainly influenced by changes in the proton $T_{1\rho}$, which becomes shorter with the addition of water. Since the sp^2 carbon has the largest T_{IS} the degradation in signal is large (20%) compared with the other carbon resonances. It is important to note that the results are similar when the polymer is hydrated with either H_2O or D_2O (see Table II). The insensitivity of the proton $T_{1\rho}$ to substitution of D_2O for H_2O indicates that rapid flipping motions of the added water do not dominate the proton relaxation in the rotating frame in the hydrated polymer samples. This relaxation data coupled with the observation of an essentially static

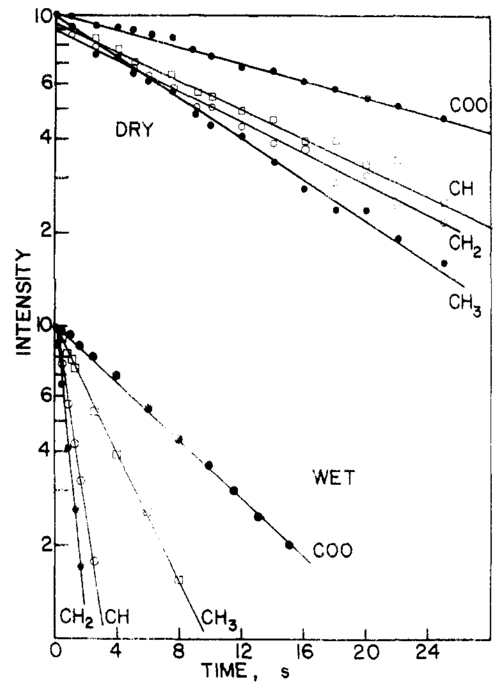

Figure 6. Representative semilogarithmic plot of the carbon-13 CP-MASS signal intensity for individual carbon atoms in dry poly(vinyl acetate) as a function of the delay time in the carbon spin–lattice relaxation time experiment.

tensor for the carboxyl carbon in these hydrated samples indicates that hydration causes an increase in low-amplitude motions of the polymer. Such small-amplitude motions do not cause a large reduction in the second moments which determine in part the T_{IS}. This conclusion is consistent with the analysis of carbon relaxation data in the rotating frame and with the changes in T_1^C observed when water is added to the polymer.

Carbon-13 Relaxation in the Zeeman Frame. Representative carbon spin–lattice relaxation data are shown in Figure 6. Within experimental error each decay may be described by a single-exponential time constant though different carbon atoms clearly have different relaxation times that range between 13 and 31 s, as summarized in Table I.

The carbon relaxation in the laboratory frame is coupled to the lattice by molecular motions and is not complicated by spin–spin effects.[26] The dominant relaxation mechanism for carbon in the solid is the modulation of the C–H dipolar interaction by molecular motion.[12,17,27-30] For the methyl carbon the rotational motion about the C_3 symmetry axis will modulate the intragroup dipolar interaction with directly bonded protons and provide a relaxation path. The long carbon T_1 for the methyl resonance demonstrates that the methyl motion is very rapid and actually in the limit $\omega_{0C}\tau_g \ll 1$, where τ_g is the correlation time for the reorientation of the methyl group. Since the motion of the methyl group is anisotropic, the carbon relaxation rates should be anisotropic and depend on the angle that the symmetry axis makes with the magnetic field direction.[17,31] For an amorphous material this effect would result in a distribution of relaxation rates spanning approximately a factor of 3,[30] but the motion of the rotor at the magic angle collapses this distribution. The powder-averaged relaxation rate for the present case is presented in ref 17 with the appropriate spectral densities. With standard values of 1.1 Å for the C–H distance within the methyl rotor and tetrahedral bond angle, the correlation time for the methyl group motion was calculated to be 2.3 ps. The extremely rapid methyl rotation is presumably made possible be a very low activation barrier created by absence of significant steric constraints in the polymer.[32]

The contribution to the sp^2-carbon relaxation from methyl rotation is estimated to be approximately 1.2×10^{-3} s^{-1} (T_1 of 850 s), which is clearly minor compared with the measured relaxation rate of 0.03 s^{-1} (30 s for T_1). Similar arguments for dominance of motions other than methyl rotations follow for the main-chain carbon atoms. Considering the observation of an essentially rigid-lattice line shape for the sp^2 carbon atom, the motion responsible for the carbon spin–lattice relaxation must leave this tensor unperturbed on the time scale of fractions of a millisecond. Thus, the high-frequency motions responsible for the longitudinal relaxation rates observed must be of small amplitude. The carbon spin–lattice relaxation times for the main-chain carbon atoms are very similar as shown in Table I. The proton environment of these carbon atoms is similar, implying that the strength of the relaxation interaction will be similar. The methyl protons are not particularly close to those carbon atoms, suggesting that carbon spin–lattice relaxation is dominated by main-chain motions, which must be of small amplitude to be consistent with the magnitude of the relaxation times and the absence of effects on the chemical shift tensors. We can provide no evidence for the ester methyl reorientations proposed earlier from dielectric relaxation measurements;[1,32] however, the powder pattern line shapes may be insensitive to rare fluctuations such as diffusion of a disturbance along the chain. It is possible that such a rare event could dominate the spin–lattice relaxation times but not affect the carbon line shapes provided that the concentration of the disturbance region is small.

Carbon-13 spin–lattice relaxation time measurements were also made on hydrated samples of poly(vinyl acetate). The results for the H_2O-treated sample are shown in Figure 6. Measurements for the D_2O-treated samples were also made and the results compared in Table I. There are significant changes in the carbon T_1 values on the addition of H_2O, but smaller changes when D_2O is used. This result is substantially different from observations of the proton and carbon relaxation times in the rotating frame (see Tables I and II).

Carbon-13 Relaxation in the Rotating Frame. Measurements of the carbon-13 relaxation in the rotating frame may provide information about motions in the mid-kilohertz range. The interpretation of the experimentally determined relaxation time for the decay of the carbon magnetization, $T_{1\rho}^{C*}$, is not simple since the carbon nuclei is the solid experience fluctuations of the local magnetic field caused by both molecular motions and spin fluctuations of the more abundant protons through their mutual static dipolar interactions. Both experimental and theoretical implications of this problem have been considered in detail for polymeric[33-44] and nonpolymeric[45-49] systems. The model appropriate for the present case has been discussed by VanderHart and Garroway.[38] The carbon-13 rotating-frame Zeeman system is coupled with the lattice via molecular motions ($T_{1\rho}^C$) and to the proton reservoir through spin–spin processes (T_{CH}^D). The proton reservoir relaxes to the lattice with a relaxation time T_{1D}^H, which under MASS conditions is usually less than 100 μs so that the condition $T_{CH}^D \gg T_{1D}^H$ is satisfied. Therefore, the carbon-13 rotating-frame magnetization will be depleted through the $T_{1\rho}^C$ path to the lattice or by relaxation via the T_{CH}^D path to the proton reservoir. Consequently, the measured $T_{1\rho}^{C*}$ may be written

$$\frac{1}{T_{1\rho}^{C*}} = \frac{1}{T_{CH}^{D}} + \frac{1}{T_{1\rho}^{C}} \qquad (4)$$

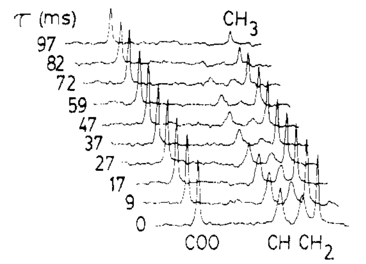

Figure 7. Carbon-13 CP-MASS spectra obtained at 14.2 MHz on dry poly(vinyl acetate) as a function of the carbon-13 spin-locking time at a locking field of 91 kHz.

A measurement of $T_{1\rho}^{C*}$ thus contains a mixture of these two effects and, therefore, a quantitative separation of spin-lattice effects from spin-spin effects is necessary before conclusions about molecular motions in the polymer may be drawn. Since our measurements are done on a sample under the MASS condition where the rotor frequency is considerably larger than $(T_{1\rho}^{C*})^{-1}$ itself, the measured values of $T_{1\rho}^{C*}$ correspond to the powder average of $T_{1\rho}^{C*}$'s for different molecular orientations. Calculation of T_{CH}^{D} for glassy polymer systems has been at best qualitative because of the difficulty in evaluating the correlation time for the proton spin fluctuations.[40,41,45-46] Moreover, an independent measurement of T_{CH}^{D} is not possible under MASS conditions when $T_{1D}^{H} \ll T_{CH}^{D}$, which is applicable in polymer systems. Recently, Schaefer and co-workers suggested a nine-step procedure for estimating the importance of T_{CH}^{D}.[43] The effects are separable if measurements are made at different spin-locking fields and if the field dependence of $T_{1\rho}^{C}$ is functionally different from that of T_{CH}^{D}. Exponential dependence of T_{CH}^{D} on the spin-locking field has been verified for crystalline L-alanine[49] and for oriented crystalline polyethylene[38] by measurements as a function of spin-locking field strength. Whereas the correlation function for the motional processes is usually assumed to be exponential, leading to a Lorentzian spectral density function,[12] the correlation function for the spin-spin fluctuations is assumed to be Lorentzian, leading to an exponential spectral density function.[45,46] For dry poly(vinyl acetate) at room temperature (295 K), information about the nature and time scale of motions is available from the proton relaxation dispersion measurements and the carbon line shape studies presented earlier. We have noted that (1) methyl rotation is very rapid ($\omega_{0C}\tau_g \ll 1$), (2) the side chain is effectively rigid as evident from an unaveraged carboxyl carbon chemical shift tensor, and (3) main-chain small-amplitude motions in the submicrosecond range apparently dominate relaxation times of all the carbon atoms. At low values of spin-locking fields (25–45 kHz), which compare with the magnitudes of the proton–carbon dipolar interactions that are modulated by the proton spin fluctuations,[45,46] the spin-locking field dependence for the spin–spin process is expected to be much stronger than for the spin–lattice processes.

Figure 7 shows the decay of the carbon intensities as a function of the spin-locking time in the CP–MASS spectra at a spin-locking field of 91 kHz. These data and those obtained at other spin-locking fields are well represented by an exponential decay. Representative data taken at 83 kHz for the spin-locking field are shown in Figure 8. The results of the $T_{1\rho}^{C*}$ measurements as a function of the spin-locking field (25–98 kHz) are shown in Figure 9 for dry poly(vinyl acetate). For each carbon there is a sharp exponential dependence at low spin-locking field strengths and either a weak or no dependence at high spin-locking fields over the range accessible. The spin–spin process may be described by the equations[38,45,48]

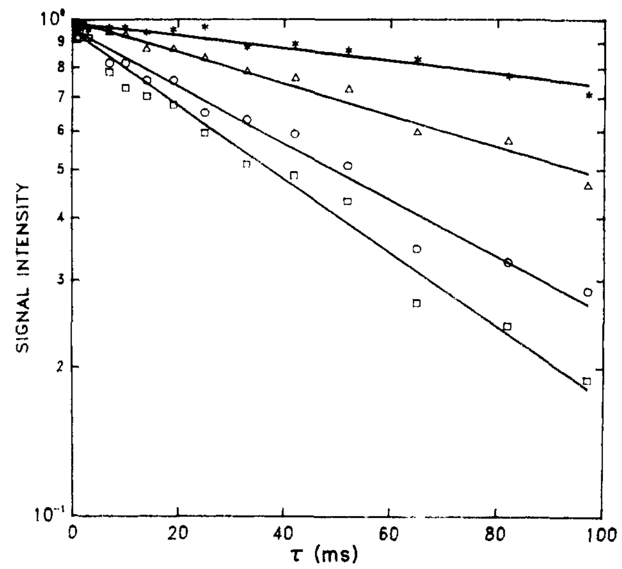

Figure 8. Semilogarithmic plots of the carbon-13 CP–MASS signal intensities for COO (*), CH (○), CH$_2$ (□), and CH$_3$ (△) carbon atoms in dry poly(vinyl acetate) as a function of the carbon spin-locking time at a spin-locking field ν_{1C} = 83 kHz which yield the decay constant $T_{1\rho}^{C*}$.

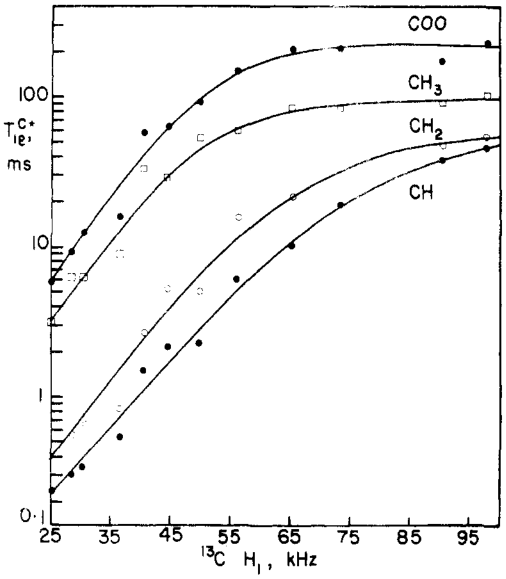

Figure 9. dependence of the apparent carbon rotating-frame relaxation time, $T_{1\rho}^{C*}$, for individual carbon atoms in dry poly(vinyl acetate) obtained at ambient probe temperatures. The solid lines are drawn through $T_{1\rho}^{C*}$ data to show the strong exponential dependence at low spin-locking fields. Analysis of the data at low spin-locking fields (25–45 kHz) leads to the cross-relaxation parameters shown in Table III.

$$\frac{1}{T_{CH}^{D}} = M_{CH}^{2} J_{D}(\omega_{1C})$$

with

$$J_{D}(\omega) = (1/2)\pi\tau_{D} \exp(-\omega\tau_{D}) \qquad (5)$$

where $2\pi\nu_{1C} = \gamma_C H_{1C}$ is the spin-locking field experienced by the carbon, M_{CH}^{2} is the second moment of the carbon nucleus in question that arises from dipolar interactions with surrounding protons, and τ_D is the correlation time of the dipolar fluctuations. A least-squares analysis of the data in Figure 9 at low spin-locking fields (25–45 kHz)

Table III
Cross-Relaxation Parameters Determined for the Spin–Spin Process to the Rotating-Frame Carbon-13 Relaxation of Dry Poly(vinyl acetate)[a]

parameter	COO	CH	CH_2	CH_3
$M_{CH}{}^2$ Hz^2	1.2×10^8	21.2×10^8	29.7×10^8	2.22×10^8
τ_D, μs	20.0	18.2	19.9	19.5

[a] Determined by analyzing the observed $T_{1\rho}{}^{C*}$ data in the range ν_{1C} = 25–45 kHz using eq 5.

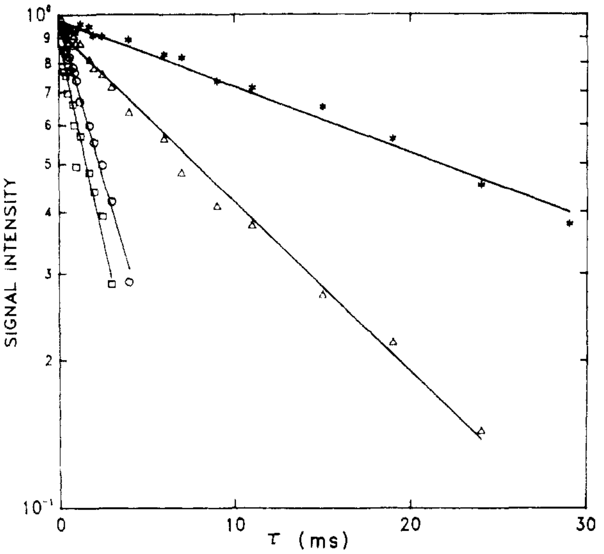

Figure 10. Semilogarithmic plots of carbon-13 CP-MASS signal intensities for COO (*), CH (○), CH_2 (□), and CH_3 (△) carbon atoms in poly(vinyl acetate) hydrated with H_2O as a function of the carbon spin-locking time at a spin-locking field of ν_{1C} = 83 kHz which yield the decay constant $T_{1\rho}{}^{C*}$.

yields the parameters $M_{CH}{}^2$ and τ_D associated with each carbon. The results are summarized in Table III, which demonstrates that the second moments, $M_{CH}{}^2$, are different for each carbon atom as expected. On the other hand, the time constant τ_D for the dipolar flip-flop correlation time of protons at each carbon atom are the same, which suggests that the simple model originally derived for simpler crystalline materials[45,48] is sufficient.[38,49]

Figure 9 indicates that spin–lattice effects dominate when the spin-locking field is greater than 75 kHz. However, at spin-locking fields less than this value where spin–spin and spin–lattice effects are mixed, the relative contribution of the spin–spin process, which scales with the second moment of the carbon–proton dipolar interaction, for the side-chain carbons is smaller than for the main-chain carbons (see Table III). At high spin-locking fields, relaxation of main-chain carbon atoms is dominated by motions of sufficiently small amplitude that the carboxyl chemical shift tensor senses only minor, if any, changes. For the methyl carbon, the observed values are several orders of magnitude smaller than that predicted from a consideration of methyl rotation alone; thus, relaxation at this carbon atom is also dominated by low-frequency small-amplitude motions of the main chain. The efficient relaxation of the main-chain carbon atoms is consistent with this interpretation because the C–H dipolar interactions are larger for these carbons with directly attached protons, which may compensate for any decrease in motional amplitude because of main-chain constraints.

Figure 10 shows the carbon-13 signal intensity decay in the CP-MASS spectrum as a function of the spin-locking time at ν_{1C} = 83 kHz for hydrated (H_2O) poly(vinyl acetate). The rotating-frame carbon relaxation data are presented in Figure 11 as a function of the spin-locking field in the same range ν_{1C} = 25–98 kHz. Compared with similar data for dry poly(vinyl acetate) (Figure 9), it is clear that the carbon relaxation time is a factor of approximately 10 smaller than that for the dry sample at very high spin-locking fields where motional effects dominate. By comparison, the differences are much smaller at the lowest spin-locking field where spin–spin effects dominate. It is clear from Figure 11 that the spin-locking frequency dependence of $T_{1\rho}{}^{C*}$ at low spin-locking fields is not simply exponential as implied by eq 5. Rather a gradual increase in $T_{1\rho}{}^{C*}$ values to a limiting plateau value is observed for all the carbons. The exponential dependence at low fields is overcome in the wet case by spin–lattice effects apparently driven by increased polymer motions. Similar measurements were made at 80 and 92 kHz for the carbon spin-locking fields when the polymer was treated with D_2O. At these spin-locking fields the spin–lattice effects dominate and within the measurement error the values are similar to those found for the samples hydrated with H_2O. Compared with the carbon Zeeman spin–lattice relaxation data these results demonstrate that low-frequency motions in the polymer dominate the carbon rotating-frame relaxation. The data for both dry and wet poly(vinyl acetate) demonstrate the importance of the dipolar interactions for carbon relaxation in the rotating frame.

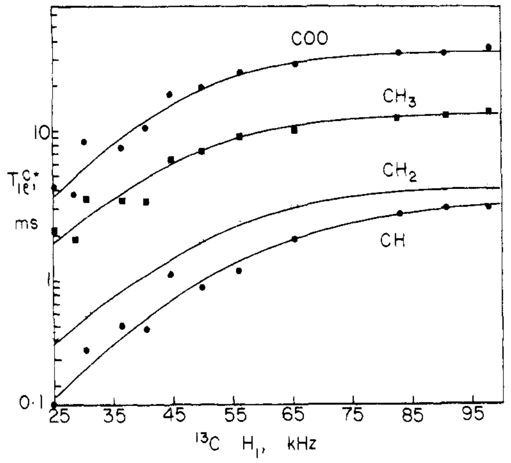

Figure 11. Apparent carbon relaxation time in the rotating frame plotted as a function of the spin-locking field strength for poly(vinyl acetate) treated with H_2O. The solid line is drawn through $T_{1\rho}{}^{C*}$ data to show a much weaker exponential dependence at low spin-locking fields.

The data summarized in Tables I and II demonstrate several fundamentally interesting aspects of water behavior in this system. The proton $T_{1\rho}$ values show that while there is a factor of 6 or more change on the inclusion of water, there is very little difference between H_2O and D_2O though the proton and deuterium magnetic moments differ by approximately a factor of 6. Similar results were found for the carbon rotating-frame measurements. Therefore, water motion itself does not contribute significantly to the low-frequency relaxation, which is apparently dominated by polymer motions. The high frequencies sensed by the carbon spin–lattice relaxation, on the other hand, show marked differences between dry and H_2O- and D_2O-treated samples (see Table I). Compared with the changes induced by H_2O, the changes caused by D_2O are small. The larger shifts in the carbon T_1 for the protonated carbon atoms are consistent with some increase in polymer motion sensed better by the $T_1{}^C$ data. The changes induced by H_2O, however, are large for all carbon atoms and demonstrate that even the carbon relaxation is dominated by dipole–dipole interactions modulated by high-frequency motions of water. This result is interesting given the low water content of the system but is consistent with other studies of water dynamics in low-water-content systems.[47]

In summary, the relaxation parameters sensitive to the lower frequencies are dominated by motions of the polymer, but these motions are sufficiently small in amplitude that the side-chain sp^2-carbon chemical shift tensor is affected very little. The relaxation parameters that sample high-frequency motions are very sensitive to the addition of water, which besides changing the polymer motions affects the carbon relaxation times directly by a dipole–dipole mechanism. The water in this polymer matrix thus has significant components at the carbon Larmor frequency and moves very rapidly in spite of the low concentration and apparent lack of fluidity in the sample.

Acknowledgment. We acknowledge with pleasure useful discussions with Professor Wilmer G. Miller and Dr. Jacob Schaefer about several aspects of this work. We thank Dr. Jersey Szumowski for several discussions and Dr. Robert Skarjune for supplying the computer program to analyze cross-polarization rates. We also thank Soctt D. Kennedy for assistance with the NMRD measurements. This work was supported by Grants from the National Science Foundation (PCM-8408620) and the National Institutes of Health (GM-34541).

Registry No. Poly(vinyl acetate) (homopolymer), 9003-20-7; water, 7732-18-5.

References and Notes

(1) McCall, D. W. *Acc. Chem. Res.* **1971**, *4*, 223.
(2) McBrierty, V. J. *Polymer* **1974**, *15*, 503.
(3) Veksli, Z.; Miller, W. G. *Macromolecules* **1977**, *10*, 686.
(4) Banks, L.; Ellis, B. *Polym. Bull.* **1979**, *1*, 377.
(5) Ford, W. T.; Balakrishnan, T. *Macromolecules* **1981**, *14*, 284.
(6) Blum, F. D.; Dickson, J. E.; Miller, W. G. *J. Polym. Sci., Polym. Phys. Ed.* **1984**, *22*, 211.
(7) Jelinski, L. W.; Dumais, J. J.; Stark, R. E.; Ellis, T. S.; Karasz, F. E. *Macromolecules* **1983**, *16*, 1019.
(8) Pines, A.; Gibby, M. G.; Waugh, J. S. *J. Chem. Phys.* **1973**, *59*, 569.
(9) Andrew, E. R.; Bradbury, A.; Eades, R. G. *Nature (London)* **1958**, *182*, 1659.
(10) Lowe, I. J. *Phys. Rev. Lett.* **1959**, *2*, 285.
(11) Schaefer, J.; Stejskal, E. O. *J. Am. Chem. Soc.* **1976**, *98*, 1031.
(12) Schaefer, J.; Stejskal, E. O. In "Topics in Carbon-13 NMR Spectroscopy"; Levy, G. C., Ed.; Wiley-Interscience: New York, 1974; Vol. I, Chapter 4.
(13) Kennedy, S. D. M.S. Thesis, University of Minnesota, Minneapolis, MN, 1984.
(14) Ganapathy, S.; Chacko, V. P.; Bryant, R. G. *J. Magn. Reson.* **1984**, *57*, 239.
(15) Hartmann, S. R.; Hahn, E. L. *Phys. Rev.* **1962**, *128*, 2042.
(16) Torchia, D. A. *J. Magn. Reson.* **1978**, *30*, 613.
(17) Naito, A.; Ganapathy, S.; Kasaka, K. A.; McDowell, C. A. *J. Magn. Reson.* **1983**, *54*, 226.
(18) Bloembergen, N.; Purcell, E. M.; Pound, R. V. *Phys. Rev.* **1948**, *73*, 679. Kubo, R.; Tomita, K.; *J. Phys. Soc. Jpn.* **1954**, *9*, 888.
(19) Gronski, W.; Nobulmichi, M. *Makromol. Chem.* **1978**, *179*, 1509.
(20) Schaefer, J. *Macromolecules* **1973**, *6*, 882.
(21) Jeener, J.; Broekaert, P. *Phys. Rev.* **1967**, *157*, 232.
(22) Goldman, M. "Spin Temperature and Nuclear Magnetic Resonance in Solids"; Clarendon Press: Oxford, 1970.
(23) Opella, S. J.; Frey, M. H. *J. Am. Chem. Soc.* **1979**, *101*, 5854.
(24) Dutch, M. W.; Grant, D. M. *Macromolecules* **1970**, *3*, 165.
(25) Mehring, M. *NMR Basic Prin. Prog.* **1976**, *11*.
(26) Schaefer, J.; Stejskal, E. O.; Buchdahl, R. *Macromolecules* **1975**, *8*, 291.
(27) Fyfe, C. A.; Lyerla, J. R.; Yannoni, C. S. *Acc. Chem. Res.* **1982**, *15*, 208.
(28) Jelinski, L. W.; Dumais, J. J.; Watnick, P. I.; Engel, A. K.; Sefcik, M. D. *Macromolecules* **1983**, *16*, 409.
(29) Akasaka, K.; Ganapathy, S.; McDowell, C. A.; Naito, A. *J. Chem. Phys.* **1983**, *78*, 3567.
(30) Gibby, M. G.; Pines, A.; Waugh, J. S. *Chem. Phys. Lett.* **1972**, *16*, 296.
(31) Torchia, D. A.; Szabo, A. *J. Magn. Reson.* **1982**, *49*, 107.
(32) Hoch, M. J. R.; Bovey, F. A.; Davis, D. D.; Douglass, D. C.; Falcone, D. R.; McCall, D. W.; Slichter, W. P. *Macromolecules* **1971**, *4*, 712.
(33) Schaefer, J.; Stejskal, E. O.; Buchdahl, R. *Macromolecules* **1977**, *10*, 384.
(34) Garroway, A. N.; Moniz, W. B.; Resing, H. A. *Org. Coat. Plast.* **1976**, *36*, 133.
(35) Stejskal, E. O.; Schaefer, J.; Steger, T. R. *Faraday Symp. Chem. Soc.* **1978**, *13*, 56.
(36) Garroway, A. N.; Moniz, W. B.; Resing, H. A. *Faraday Symp. Chem. Soc.* **1978**, *13*, 63.
(37) Garroway, A. N. *J. Magn. Reson.* **1979**, *34*, 283.
(38) VanderHart, D. L.; Garroway, A. N. *J. Chem. Phys.* **1979**, *71*, 2773.
(39) Veeman, W. S.; Menger, E. M.; Ritchey, W.; de Boer, E. *Macromolecules* **1979**, *12*, 924.
(40) Cheung, R. R. P.; Yaris, R. *J. Chem. Phys.* **1980**, *72*, 3604.
(41) Garroway, A. N.; VanderHart, D. L.; Earl, W. L. *Philos. Trans. R. Soc. London, Ser. A* **1981**, *299*, 609
(42) Schaefer, J.; Sefcik, M. D.; Stejskal, E. O.; McKay, R. A.; Dixon, W. T.; Cais, R. E. *Macromolecules* **1984**, *17*, 1107.
(43) Schaefer, J.; Sefcik, M. D.; Stejskal, E. O.; McKay, R. A. *Macromolecules* **1984**, *17*, 1118.
(44) Laupretre, F.; Monnerie, L. *Macromolecules* **1984**, *17*, 1397.
(45) McArthur, D. A.; Hahn, E. L.; Walstedt, R. E. *Phys. Rev.* **1969**, *188*, 609.
(46) Demco, D. E.; Tegenfeldt, J.; Waugh, J. S. *Phys. Rev. B* **1975**, *11*, 4133.
(47) Pines, A.; Shattuck, T. W. *J. Chem. Phys.* **1974**, *61*, 1255.
(48) Stokes, H. T.; Ailion, D. C. *Phys. Rev. B* **1977**, *15*, 1271.
(49) Akasaka, K.; Ganapathy, S.; McDowell, C. A.; Naito, A. *J. Chem. Phys.* **1983**, *78*, 3567.
(50) Shirley, W. M.; Bryant, R. G. *J. Am. Chem. Soc.* **1982**, *104*, 2910.
(51) Kaplan, J. I.; Garroway, A. N. *J. Magn. Reson.* **1982**, *49*, 464.